Carrier-induced shift and broadening of optical spectra in an $Al_xGa_{1-x}As/GaAs$ quantum well with a gate electrode

H. Yoshimura
Institute of Industrial Science, University of Tokyo, 7-22-1 Roppongi, Minato-ku, Tokyo 106, Japan

G. E. W. Bauer
Philips Research Laboratories, NL-5600 JA Eindhoven, The Netherlands

H. Sakaki
Institute of Industrial Science, University of Tokyo, 7-22-1 Roppongi, Minato-ku, Tokyo 106, Japan
(Received 16 February 1988; revised manuscript received 23 May 1988)

We have investigated the carrier-induced changes in the photoluminescence (PL) and excitation spectra (PLE) of an *n*-type $Al_xGa_{1-x}As/GaAs$ quantum-well structure at 10 K by controlling the electron concentration ($N_s=0-10^{12}$ cm^{-2}) via gate electric fields. By comparison with local-density-functional theory, the red shift of the PL peak and the blue shift of the PLE spectra could be ascribed to band-gap renormalization (~ 18 meV at $N_s=1\times10^{12}$ cm^{-2}) and to band-filling effect. While appreciable portions of the PL and the PLE linewidths are attributed to thermal broadening, the presence of additional broadening is noted and discussed in terms of the localization of carriers, the Auger effect, and other mechanisms.

I. INTRODUCTION

Semiconductor quantum-well (QW) structures possess unique optical properties, including a strong exciton contribution to the interband transition[1] and a distinctive shift of the absorption edge caused by transverse electric fields.[2,3] Optical properties of QW's are strongly modified when carriers are introduced into the well.[1,4–14] For example, the absorption spectra are affected by the presence of carriers through such mechanisms as (1) quenching of excitonic absorption caused by phase-space filling and screening,[1] (2) band-gap renormalization due to particle correlations,[1,5–9,14] (3) the Burstein-Moss shift due to band filling,[5,9] and (4) Fermi-surface singularity due to the correlation between a photoexcited hole and Fermi-sea electrons.[10,11] Furthermore, the presence of carriers may modify the optical spectra through (5) the Auger effect (AE) (Refs. 14 and 15) and (6) the possible formation of tail states or the localized states near the band edge. Carrier-induced changes in refractive index have also been pointed out.[13,16]

Although these carrier-induced optical effects have been studied mainly by introducing carriers through optical excitation,[4,10,14] current injection,[6] or modulation doping,[5,7–9,11] some experiments have been recently made in which the electron concentration in a quantum well is varied by using a field-effect-transistor (FET) configuration. This scheme has been applied to optical read out of the logic state of an FET.[12] The application of this QW FET to a waveguide optical modulator of absorption type has been proposed and analyzed to show its high potential for application.[12,13,16,17]

QW FET's of this kind are important not only for these applications, but are ideal systems for the study of carrier-induced optical effects since the concentrations N_s and the temperatures T_e of electrons can be accurately controlled in a single sample.[12,18] Indeed, Bar-Joseph *et al.*[18] and Delalande *et al.*[19] have recently adopted such an approach. The former performed modulation spectroscopy of the optical absorption of an $In_{1-x}Al_xAs/In_yGa_{1-y}As$ FET. The latter measured the photoluminescence (PL) and photoluminescence excitation spectra (PLE) of an $Al_xGa_{1-x}As/GaAs$ FET. Both of them observed energy shifts and a change of excitonic absorption as functions of the electron concentration and interpreted them in terms of mechanisms (1)–(3).

In this study, we report on measurements of PL and PLE of $GaAs/Al_xGa_{1-x}As$ single-QW FET structure with N_s being scanned from 0 to 1×10^{12} cm^{-2}. We compare the experimental data of the spectral shift with local-density-functional theory[8] and evaluate separately the relative contributions of the many-body effect, the band-filling effect, the Stark effect, and other carrier-induced effects. We examine also the mechanisms responsible for the PL and PLE linewidths.

II. SAMPLE PREPARATION AND EXPERIMENTALS

An *n*-type $Al_xGa_{1-x}As/GaAs$ modulation-doped QW used in this study was grown on semi-insulating (100) GaAs by molecular-beam epitaxy. As shown in Fig. 1(a), we grew successively 5000 Å undoped GaAs, five periods of GaAs(30 Å)/$Al_xGa_{1-x}As$(30 Å) superlattice buffer, 2000 Å undoped $Al_xGa_{1-x}As$, 120 Å GaAs QW, 50 Å undoped $Al_xGa_{1-x}As$ spacer layer, 600 Å *n*-type $Al_xGa_{1-x}As$ layer with the donor (Si) concentration of 5×10^{17} cm^{-3} and 100 Å GaAs cap layer. The Al mole fraction of all the $Al_xGa_{1-x}As$ layers is 0.3. The elec-

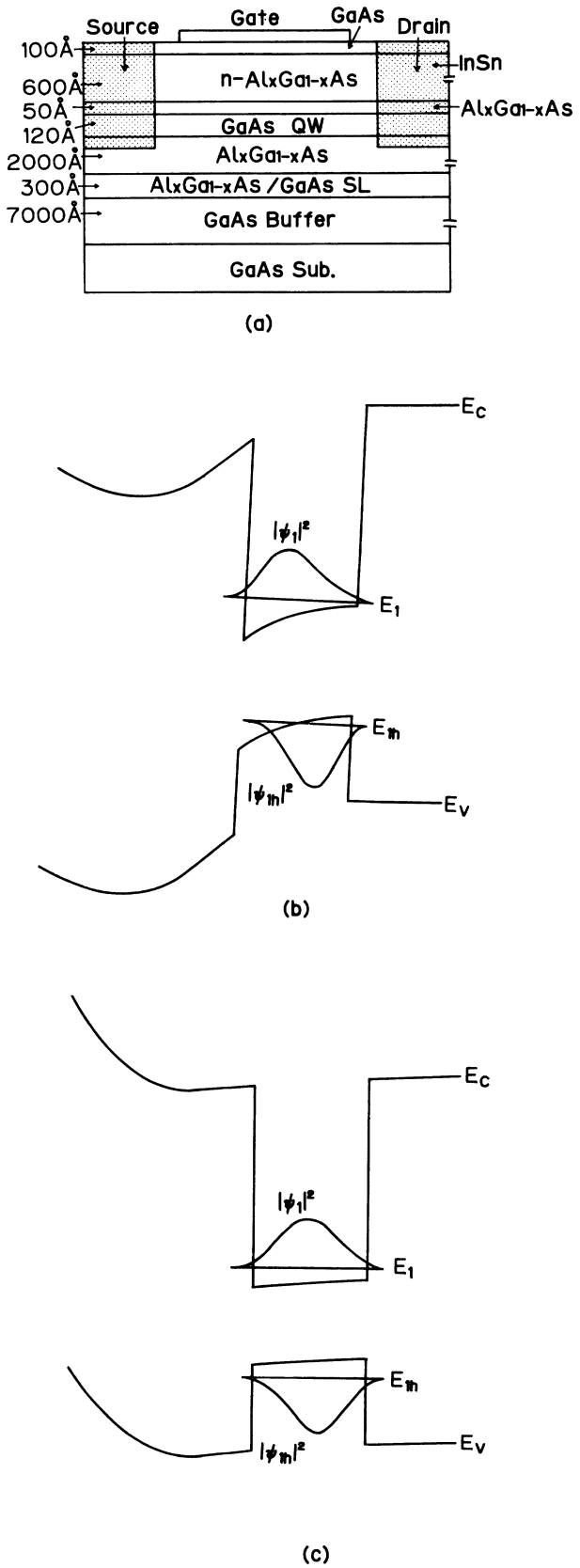

FIG. 1. The schematic structure of quantum-well FET (a) and the band bendings (b) and (c) at high and low electron concentrations.

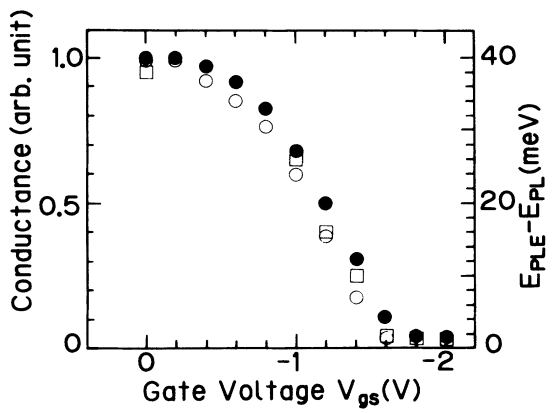

FIG. 2. The source-drain conductance measured under weak room-light illumination is plotted by open circles and that under illumination of He-Ne laser by closed circles. The energy difference between PL and PLE is also shown by open squares.

tron concentration N_s is 1×10^{12} cm^{-2} and the mobility μ is 74 000 cm^2/V sec at 77 K under light illumination.

To fabricate depletion mode QW FET's, InSn was deposited and patterned to form the source-drain electrodes and alloyed at 400 °C for 1 min. A semitransparent 200-Å-thick Au gate electrode of 2×3 mm^2 was formed. Figures 1(a), 1(b), and 1(c) show, respectively, the sample structure and the band bendings for high and low electron concentrations. Figure 2 shows the source-drain

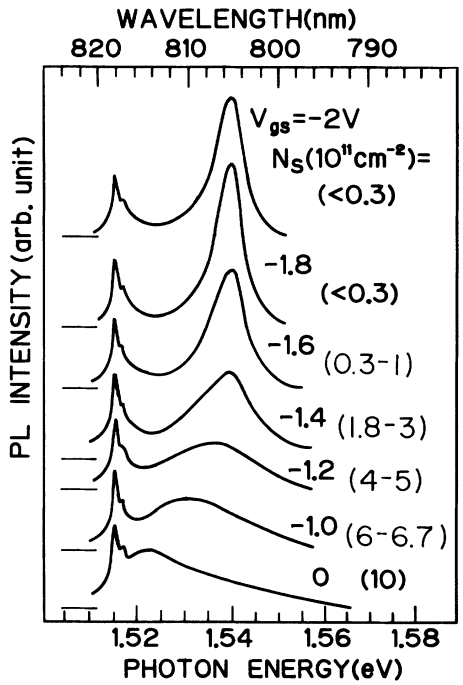

FIG. 3. Photoluminescence spectra of the n-type $Al_xGa_{1-x}As/GaAs$ single quantum well ($L_w=120$ Å) at various electron concentrations, $N_s=0-1\times10^{12}$ cm^{-2} controlled by gate electric fields.

conductance of the FET measured at 77 K as a function of the gate voltage V_{gs}. Open circles are the data taken under a weak room-light illumination and closed circles are under the illumination of He-Ne laser ($\lambda=6328$ Å, $P=1$ W/cm^2). Note that FET action is achieved in both cases. The conductance is constant when $0>V_{gs}>-0.2$ V, but decreases almost linearly as V_{gs} is made more negative, reaching nearly zero at -2 V. Although the PL and PLE measurements were done at 10 K under the illumination with the wavelength of 7600 Å and 7600–8100 Å, respectively, the FET action during these measurements is considered to be quite close to that of Fig. 2, since the V_{gs} dependence of N_s is independent of temperature for $T<100$ K and the excitation light used in our PL and PLE measurement generates only a small number of carriers.

The PL spectra and the PL excitation spectra were measured at 10 K by using the Styryl-8 dye laser pumped by the cw Ar laser. The excitation area was about 100×100 μm^2, and the power density is 10 W/cm^2. Figures 3 and 4 show the PL and the PLE spectra at different gate voltages V_{gs}. The estimated electron concentration $N_s(V_{gs})$ at each of these gate voltages in units of 10^{11}/cm^2 is $N_s<0.3$ at $V_{gs}=-2$ V, <0.3 at -1.8 V, 0.3–1 at -1.6 V, 1.8–3 at -1.4 V, 4–5 at -1.2 V, 6–6.7 at -1.0 V, and 10 at 0 V. The sharp PL peaks observed at $\lambda=8180$ Å and 8172 Å in Fig. 3 originate from the GaAs buffer layer. The broader PL peak on the higher-energy side comes from the QW and shifts by about 17.5 meV towards lower energy when N_s increases. The PLE spectra in Fig. 3 exhibit a well-resolved excitonic peak in the region of low N_s ($<3\times10^{10}$ cm^{-2}). For higher N_s, the quenching of excitons and the blue shift of the absorption edge are clearly observable.

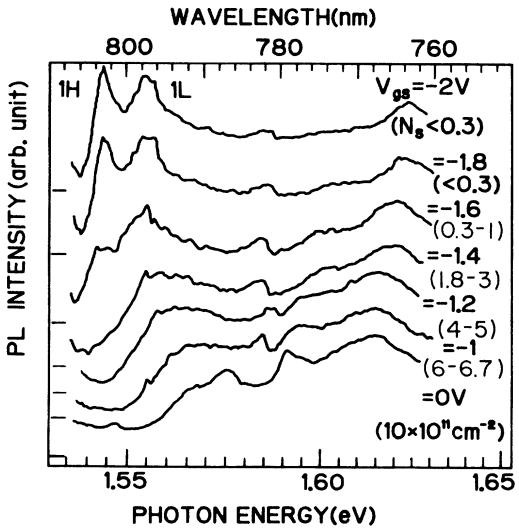

FIG. 4. Photoluminescence excitation spectra of the n-type $Al_xGa_{1-x}As/GaAs$ single quantum well ($L_w=120$ Å) at various electron concentrations; $N_s=0-1\times10^{12}$ cm^{-2} controlled by gate electric fields.

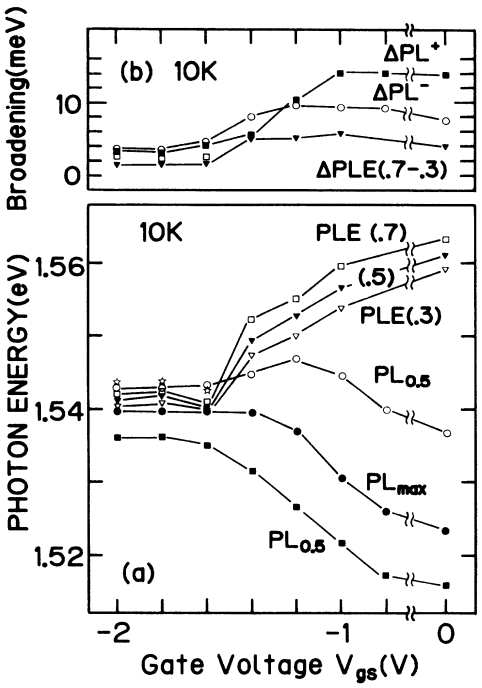

FIG. 5. The gate voltage dependence (carrier concentration dependence) of photoluminescence (PL) and excitation (PLE) spectra (a) and their widths (b). The solid circles in the lower figure (a) show the PL peak E_{PL}^{max}, while the solid squares and open circles show the photon energies $E_{PL}^{max}-\Delta_{PL}^{-}$ and $E_{PL}^{max}+\Delta_{PL}^{+}$ at which the PL intensity is reduced to 50% of its maximum. Also shown by open triangles, solid triangles, and open squares are the photon energies $E_{PLE}(0.3)$, $E_{PLE}(0.5)$, and $E_{PLE}(0.7)$ at which the PLE intensity is 30%, 50%, and 70% of the first PLE step or of the excitonic peak (see text for details). The exciton peak energy is also shown at $V_{gs}<-1.6$ V (open stars). Upper figure (b) shows the gate voltage dependence of the PL half-width at half maximum on the lower-energy side (open circles) and that on the higher-energy side (solid squares). Also shown by solid triangles is the energy difference between $E_{PLE}(0.7)-E_{PLE}(0.3)$. Shown by open squares are the half-widths at half maximum on the lower-energy side of the heavy-hole exciton peak of PLE.

In Figs. 5(a) and 5(b) we plot the peak position E_{PL}^{max} and the linewidths of the PL spectra as functions of gate voltage. For PLE spectra, we plot in Fig. 5(a) the three photon energies $E_{PLE}(0.3)$, $E_{PLE}(0.5)$, and $E_{PLE}(0.7)$ at which the intensity of the PLE spectra reaches 30%, 50%, and 70% of their maxima, which is defined as the height of the first PLE step for $V_{gs}\geq-1.4$ V and as the height of the heavy-hole excitonic peak for $V_{gs}\leq-1.6$ V.

III. CARRIER-INDUCED SHIFTS OF PL AND PLE SPECTRA

A. Shift of PL spectra and band-gap renormalization

The red shift of the PL peak shown in Fig. 3 is caused by a many-body effect usually referred to as band-gap renormalization[19] and by the modified Stark effect in the

presence of carriers. As illustrated in Figs. 1(b) and 1(c) the electric field at the front heterointerface increases linearly with $(N_s+N_{\rm dep})$, where $N_{\rm dep}$ is the concentration of the depletion-layer charge ($<1\times10^{11}$ cm^{-2}). By using local-density-functional theory[8] which takes into account both the many-body effect and the band bending effect, we have calculated the ground level E_1 of electrons and that of heavy holes E_{1h}. The effective energy gap E_g^*, which is defined as the energy separation between E_1 and E_{1h}, can be also calculated. Its shift is predicted to be 26.7 meV as N_s is changed from zero to 1×10^{12} cm^{-2}. Since the PL peak is dominated by free-carrier recombination at high-electron concentration and becomes excitonic at low N_s, the PL peak energy $E_{\rm PL}^{\rm max}$ is equal to E_g^* only at high N_s, but is equal to $(E_g^*-E_b)$, where E_b is the exciton binding energy at low N_s. If we take this correction term, which is calculated to be 9 meV in this case, into account only at low-carrier concentration, the shift of PL energy is predicted to be 17.7 meV (=26.7 meV -E_b). This is very close to the observed shift ($\sim$17.5 meV). In other words, our experiment has indicated that the shift of the effective energy gap E_g^* is 26.5 meV (=17.5 meV + E_b).

To clarify the relative importance of the many-body effect and the Stark effect, we have performed the energy-level calculation in the Hartree approximation which takes into account only the self-consistent band bending effect. The shift of the effective energy gap E_g^* is then predicted to be 8.5 meV which corresponds to a PL energy shift of -0.5 meV ($=8.5$ meV$-E_b$). Hence, the observed energy-gap shift 26.5 meV at $N_s=1\times10^{12}$ cm^{-2} can be mainly ascribed to the many-body effect ($\sim$18.2 meV) and partly to the Stark effect ($\sim$8.5 meV). The deduced band-gap shrinkage (18.2 meV) due to the many-body effect is much smaller than that reported by Trankle *et al.*;[14] he found that the shrinkage was 40 meV when the electron-hole plasma with the carrier concentration of 10^{12} cm^{-2} was generated.[14] The many-body effect should be larger in electron-hole plasmas because the numbers of particles is twice as large for the same density. But this does not explain the very large values of Trankle. The origin of this discrepancy is not clear but calls for further study.

B. Burstein-Moss shift

As shown in Fig. 4, the PLE spectra exhibit sharp peaks when $V_{gs}=-1.8$ V ($N_s<3\times10^{10}$ cm^{-2}), but in the region of higher electron concentrations the bleaching of excitons and a blue shift of the absorption (or PLE) edge are observed. The energy difference $\Delta h\nu$ between the PLE edge and the PL peak in that region ($N_s>3\times10^{11}$ cm^{-2}) results from the band filling by conduction-band electrons. Hence, $\Delta h\nu$ should be equal to the sum of electron Fermi energy E_F and the hole energy $E_h=E_h(k_F)$, where k_F is the Fermi momentum $(2m_eE_F)^{0.5}/\hbar$ and m_e the effective mass of the electrons. If the conduction and valence bands are assumed to be parabolic, $E_h(k_F)$ is $(\hbar^2/2m_h)k_F^2$ and $\Delta h\nu$ is given by $E_F\times(1+m_e/m_h)$ in the degenerate case, where m_h is the effective hole mass for the motion along the heterointerface. This relation suggests that $\Delta h\nu$ should depend linearly on E_F (or N_s). However, this simple treatment is not adequate here, since the valence band has a nonparabolic dispersion relation, where the heavy-hole mass at k_F gets heavier with increasing N_s. At $N_s=1\times10^{12}$ cm^{-2} or $E_F=35.7$ meV, the Fermi wave number k_F is 2.5×10^6 cm^{-1}. A calculation of the valence-band structure (neglecting the small effects due to the band bending) has shown that the energy $E_h(k_F)$ is about 4.8 meV, which corresponds to an effective hole mass of $0.5m_e$. The prediction that $\Delta h\nu$ is 40.5 meV (=35.7 meV + 4.8 meV) agrees well with the observation $\Delta h\nu=38$ meV at $V_{gs}=0$ V ($N_s=1\times10^{12}$ cm^{-2}).

We plot in Fig. 2 the energy difference $\Delta h\nu$ between the onset energy $E_{\rm PLE}(0.5)$ of PLE and the PL peak as a function of gate voltage. Note that the data (denoted by squares) show a linear increase and saturation, which follows closely the change of the channel conductance or the electron concentration. One should recall here that the exciton correction at low-electron concentration ($N_s<1\times10^{11}$ cm^{-2}) affects both the PL and PLE energy and, hence, does not appear in the difference of the two.

Note also in Figs. 3 and 5 that the position of the PL peak remains unchanged for $N_s<3\times10^{11}$ cm^{-2}. This is likely to reflect the competition between the band-gap renormalization and the quenching of the exciton. When N_s is increased from zero to a small value ($<2\times10^{11}$ cm^{-2}), the quenching of the exciton should raise the absorption edge by about $E_b\sim9$ meV, whereas the band-gap renormalization lowers the PL energy. These two factors are of the same order of magnitudes and, therefore, more or less cancel each other, and keep the PL energy constant.

IV. LINEWIDTHS OF PL AND PLE SPECTRA

The linewidths of the PL and the PLE spectra summarized in Fig. 5 contain various information on the energy and wave-number distribution of carriers as well as on the inhomogeneity of the system. We denote the half-width at half maximum of both the high-energy and low-energy side of PL by $\Delta_{\rm PL}^+$ and $\Delta_{\rm PL}^-$. Similarly, we define the broadening of PLE spectra by $\Delta E_{\rm PLE}^{(0.3\text{-}0.7)}$, which is the energy range over which the PLE intensity increases from 30% to 70% of its maximum or its full value. Note first in Fig. 5 that $\Delta_{\rm PL}^+$, $\Delta_{\rm PL}^-$, and $\Delta E_{\rm PLE}^{(0.3\text{-}0.7)}$ are all rather narrow (2–3.5 meV) when $N_s\approx0$ ($V_{gs}\le-1.8$ V) where the optical processes are excitonic. The linewidths, however, increase substantially, when N_s is raised to 1×10^{12} cm^{-2}; they show maxima at intermediate electron concentrations.

When N_s is sufficiently high, excitons are quenched and optical processes are dominated by the interaction between a large number of electrostatically induced electrons and a small number of photoexcited holes.[11,20] Hence the line shapes of PL and PLE should be affected by such factors as the energy and the wave-number distributions of electrons and/or holes. We study below such mechanisms as (1) the thermal (k_BT) broadening, (2) the correlation between photoexcited holes and electrons, (3)

the inhomogeneous broadening, and (4) the lifetime broadening[21] which all give rise to the broadening of PL and PLE. Furthermore, we discuss effects of (5) the localization of holes, (6) the Auger process,[15] and (7) the possible formation of tails in the reduced density of states. These processes may result in the breakdown of the **k** selection rule, and give rise to additional broadenings.

A. Linewidths of excitation spectra

We examine first how the PLE broadening $\Delta E_{\rm PLE}^{(0.3\text{-}0.7)}$ of Fig. 5(b) can be explained. We discuss, in particular, both the contribution from the thermal distribution of carriers and that of the correlation between photoexcited holes and Fermi-sea electrons in addition to the inhomogeneous broadening.

Suppose that the excitonic contribution is completely suppressed by a large number of free electrons, the interband absorption coefficient of an n-type QW is expressed as

$$\alpha'(h\nu)=\alpha_n(h\nu)[1-f_c(h\nu)][1-f_h(h\nu)] ,$$

where $f_c(h\nu)$ and $f_h(h\nu)$ are the Fermi-Dirac distribution function of electrons and holes in those states that are involved in the optical transitions of energy $h\nu$. The band-filling effect is expressed by $(1-f_c)(1-f_h)$ while $\alpha_n(h\nu)$ is the interband absorption spectrum in the absence of carriers. If we assume that the E-**k** relation of holes is approximated by a parabola $(\hbar^2/2m_h^*)k^2$ in the vicinity of the Fermi momentum k_F, the expected broadening $\Delta E_{\rm PLE}^{(0.3\text{-}0.7)}$ caused by the band filling of thermally distributed carriers is given by $1.7k_BT(1+m_e/m_h^*)$. At $T=10$ K (20 K), where k_BT is 0.86 meV (1.72 meV), $\Delta E_{\rm PLE}^{(0.3\text{-}0.7)}$ is predicted to be 1.7–1.8 meV (3.4–3.6 meV). In this estimation, we have taken into account that the effective hole mass $\hbar^{-2}\sigma^2E/\sigma^2k$ is strongly dependent on the wave number and is around $(0.3-0.5)m_0$ in this region.

When at intermediate electron concentration the quenching of the exciton is not complete, the absorption may be broadened by the correlation of Fermi-sea electrons and photoexcited holes. This situation is somewhat analogous to that of indirect-band-gap semiconductors[20] in the sense that the transition takes place between a valence-band state with $k=0$ and a conduction-band state with $k=k_F$. In this case, the energy and momentum conservation are ensured by the simultaneous excitation of particle-hole pairs or plasmons instead of the emission of phonons. Hence the broadening tail is at most the energy difference between the direct transition and the indirect transition, which is the kinetic energy $E_h(k_F)$ of the heavy hole in the first subbands with the Fermi wave vector k_F. This term $E_h(k_F)$ has been discussed earlier in connection with the Burstein shift and shown to be 4.8 meV at $N_s=1\times10^{12}$ cm^{-2} when the nonparabolicity of the valence band is taken into account.

The measured broadening $\Delta E_{\rm PLE}^{(0.3\text{-}0.7)}$ of Fig. 5 is 2 meV at $V_{gs}=-2$ V ($N_s\simeq0$) increases to 5–6 meV at intermediate value of N_s [$(4-6)\times10^{11}$ cm^{-2}] and then reduces to 4 meV at $V_{gs}=0$ ($N_s=1\times10^{12}$ cm^{-2}). Since the broadening at $N_s=0$ is due to the excitonic broadening and originates mainly from the inhomogeneity, the incremental broadening at intermediate and high N_s should be ascribed to those carrier-induced effects. This increment is 3–4 meV (=5–6 meV−2 meV) at $N_s=4-6\times10^{11}$ cm^{-2} and 2 meV (=4 meV−2 meV) at $N_s=10^{12}$ cm^{-2}. The former (3–4 meV) is very close to the predicted value for correlation-related broadening whereas the latter (2 meV) value can be well explained by the simple model for thermal broadening at $T=10$ K.

Even when the whole broadening 4 meV at $N_s=1\times10^{12}$ cm^{-2} is ascribed to thermal broadening, the electron temperature T_e is found to be 24 K. Therefore a rise of T_e in this experiment is quite small (<12 K). Hence the broadening of PLE spectra can be explained by these mechanisms without assuming much rise in T_e. This is different from the earlier report of Bar-Joseph *et al.*,[18] in which the measured broadening was ascribed to the rise of T_e of more than 40 K.

The exact reason for the enhanced broadening $\Delta E_{\rm PLE}^{(0.3\text{-}0.7)}=6$ meV observed at the intermediate electron concentrations ($N_s\simeq6\times10^{11}$ cm^{-2} at $V_{gs}\simeq-1.0$ V) is not clear but is likely to be associated with the correlation effect as discussed earlier, since such an effect becomes important when the electron concentration is neither too high nor too low.

One should bear in mind that there are two other mechanisms that may give rise to additional broadenings at intermediate values of N_s. First, the inhomogeneity of the gate region of the system may give rise to local fluctuations of the FET threshold voltage and the electron concentration N_s in the channel. Indeed, such an inhomogeneity is often experienced in quantum Hall-effect studies, where the Landau-level filling is usually rather inhomogeneous when controlled by gate voltage instead of magnetic field. If N_s varies by about 1×10^{11} cm^{-2} from one place to another, it should broaden the PLE spectra by 2 meV, as suggested in Fig. 5. Note that this fluctuation is reduced when the gate voltages is sufficiently high (>-0.4 V), since an electrically neutral region is formed in the n-type $Al_xGa_{1-x}As$ layer and N_s does not depend on the V_{gs} any longer.

Another mechanism that may broaden the PLE spectra in the intermediate value of N_s is the increase in the number of ionized donor impurities in the depletion region of the n-type $Al_xGa_{1-x}As$, where the depletion-layer width increases as V_{gs} is made more negative. Although further work is necessary to quantify these contributions, the enhancement of inhomogeneity by the gate electric field may well be partly responsible for the additional broadening.

B. Linewidths of photoluminescence spectra

We examine next the linewidths $\Delta_{\rm PL}^{+}$ and $\Delta_{\rm PL}^{-}$ of the PL peak on the higher-energy side and lower-energy side, respectively. In a PL measurement a small number of holes is created by optical excitation which relax to the bottom of the valence band. They are thermally distributed over the energy range of $k_BT_h\sim2$ meV, which corresponds to

a spread of wave numbers of about 1.2×10^6 cm^{-1}. On the other hand, electrons are induced by the field effect and occupy generally a wider range of k at 10 K since the Fermi-wave number k_F is given by $(2\pi N_s)^{0.5}$ under degenerate case and is 2.5×10^6 cm^{-1} when N_s is 10^{12} cm^{-2}.

The PL line shape is expressed as

$$I_{\rm PL}(h\nu)=\int M^2 p(h\nu) f_c(h\nu) f_h(h\nu)\delta(h\nu,E)dE \ ,$$

where M is the momentum matrix element, $p(h\nu)$ is the reduced density of states, and $\delta(h\nu,E)$ is the broadening function which includes the carrier-induced effect. When $N_s=10^{12}$ cm^{-2} ($V_{gs}\geq -0.4$ V), we can assume that f_c is almost 1 and that M^2 and $p(h\nu)$ are nearly constant in the energy range where the radiation occurs. Hence the PL line shape should reflect mainly the Boltzman distribution k_BT of holes and the corresponding distribution of electrons that recombine with holes. This means that PL shows an exponential tail of the form $I(h\nu)=A\exp(-h\nu/B)$ on the higher-energy side of the PL peak. Here B is the joint thermal energy constant and is expressed as $(1+m_h/m_e)k_BT$ for a parabolic case, where m_h is the effective mass of heavy holes along the QW plane near the band bottom ($\sim0.18m_0$). Considering $m_h/m_e=2.69$, B is predicted to be 3.2–6.4 meV at $T=10$ K (or 20 K). Although the nonparabolicity of hole subbands may further enhance the broadening, the prediction (3.2–6.4 meV) is far smaller than the experimental value $B=15.1$ meV obtained at $N_s=1\times10^{12}$ cm^{-2} ($V_{gs}=0$ V). Hence the major portion of the observed broadening should be ascribed to some other mechanism.

Other mechanisms that may broaden the higher-energy side of the PL peak are those that allow the recombination of holes with k much greater than their thermal values; the Coulomb enhancement near the Fermi surface, for example, enhances the optical transition near k_F as discussed in connection with the excitation spectrum. One also expects an appreciable spread of the hole wave number over a wider range in k space, if holes are localized by some inhomogeneities with an attractive potential. If the lateral size of such a localized state is 300 Å, the hole wave number may spread to 2×10^6 cm^{-1}. This corresponds to the kinetic energy of 3.6 meV for holes and 22.8 meV for electrons. Such a spread is large enough to explain the broadening constant B of about 15 meV. In fact, the Coulomb enhancement near the Fermi surface and the hole localization may function additively. Similarly, any inhomogeneities which break the k selection rule may also cause broadenings.

The linewidth data of Fig. 5 show that $\Delta_{\rm PL}^-$ on the low-energy side of the PL peak increases from 3.6 to 7.8 meV, as N_s is increased from zero to 1×10^{12} cm^{-2}. Such a large broadening cannot be explained by the lifetime broadening,[21] because the measured mobility at $N_s=1\times10^{12}$ cm^{-2} is as high as 74 000 cm^2/V sec at 10 K. This corresponds to a broadening $\Delta E=(e\hbar/2m_e\mu)$ of 0.12 meV. Even when we consider that μ decreases nearly linearly with N_s^1 or $N_s^{1.5}$, and the lifetime broadening increases as N_s is reduced, the expected broadening is still less than 1 meV for $N_s>3\times10^{11}$ cm^{-2}.

Inhomogeneities in the QW system such as impurities and interface roughness may broaden the PL linewidth. In particular, the measured linewidth of $\Delta_{\rm PL}^-$ (~3.6 meV) of the excitonic PL at low temperatures at $N_s\simeq0$ ($V_{gs}=-2$ V) is likely to be dominated by such inhomogeneities. Since a heterointerface fluctuation of at least 1 monolayer is expected in MBE grown samples, this accounts for the level broadening of about 1 meV when $L_z>100$ Å. The remaining portion of the broadening (2.6 meV$\approx$3.6 meV -1 meV) is most probably due to the potential fluctuation caused by the donor impurities in n-type $Al_xGa_{1-x}As$ or by interface fluctuation of greater amplitudes, possibly a few monolayers. These impurity or interface related broadenings may depend on the electron concentration N_s, but are likely to decrease with increasing N_s because of screening. Hence, the contribution of impurity related broadening $\Delta_{\rm PL}^-$ in the region of high $N_s>3\times10^{11}$ cm^{-2} is estimated to be of the order of 3 meV or less.

Thus by assuming an inhomogeneity broadening of about 3 meV and a lifetime broadening of 0.2–1 meV at $N_s=1\times10^{12}$ cm^{-2}, one should still look for other mechanisms to account for the remaining portion of $\Delta_{\rm PL}^-$, which is about 3–4 meV at high N_s. This mechanism should be one that becomes important only at high N_s. Possible candidates are the Auger process of electrons and the formation of the nonparabolic tail in the joint density of states which are known to play some roles in doped semiconductors. Hence, we conclude here that the broadening due to the Auger effect[15] or to the nonparabolic tail states is small and at most 4 meV. This conclusion contradicts somewhat with the work of Trankle *et al.*,[14] since they have found that measured $\Delta_{\rm PL}^-$ becomes as large as 20 meV when electron hole pairs of about 10^{12} cm^{-2} is generated and have ascribed it mostly to Auger processes. We think that their broadening is most likely dominated by the well width fluctuation, since their well width is so thin (21 Å) that one monolayer fluctuation may broaden the PL line width by about 20 meV.

V. SUMMARY

We have studied optical properties of a modulation-doped single quantum well by controlling the electron concentration via gate electric fields. Both the red shift of the emission energy and the blue shift of the absorption edges are compared with local-density-functional theory and are ascribed to many-body effects and band filling. Mechanisms which dominate the PL and PLE linewidths are discussed and clarified.

ACKNOWLEDGMENTS

The authors wish to express sincere thanks to Professor T. Ando for stimulating discussions. This work is supported by a Grant-in-Aid from the Ministry of Education, Science and Culture, Japan. One of the authors (H.Y.) acknowledges partial financial support from the Japan Society for the Promotion of Science.

[1]D. S. Chemla and D. A. B. Miller, J. Opt. Soc. Am. B **2**, 1155 (1985).
[2]D. A. B. Miller, D. S. Chemla, T. C. Damen, A. C. Gossard, W. Wiegmann, T. H. Wood, and C. A. Burrus, Phys. Rev. B **32**, 1043 (1985).
[3]D. A. B. Miller, D. S. Chemla, T. C. Damen, A. C. Gossard, W. Wiegmann, T. H. Wood, and C. A. Burrus, Appl. Phys. Lett. **45**, 13 (1984).
[4]D. A. B. Miller, D. S. Chemla, D. J. Eilenberger, P. W. Smith, A. C. Gossard, and W. T. Tsang, Appl. Phys. Lett. **41**, 679 (1982).
[5]A. Pinczuk, J. Shah, H. L. Stormer, R. C. Miller, A. C. Gossard, and W. Wiegmann, Surf. Sci. **142**, 492 (1984).
[6]S. Tarucha, H. Kobayashi, Y. Horikowshi, and H. Okamoto, Jpn. J. Appl. Phys. **23**, 874 (1984).
[7]D. A. Kleinman and R. C. Miller, Phys. Rev. B **32**, 2266 (1985).
[8]G. E. W. Bauer and T. Ando, Phys. Rev. B **31**, 8321 (1985).
[9]M. H. Meynadier, J. Orgonasi, C. Delalande, J. A. Brum, G. Bastard, M. Voos, G. Weimann, and W. Schlapp, Phys. Rev. B **34**, 2482 (1986).
[10]S. Schmitt-Rink, C. Ell, and H. Haug, Phys. Rev. B **33**, 1183 (1986).
[11]M. Skolnick, J. M. Rorison, K. J. Nash, D. J. Mowbray, P. R. Tapster, S. J. Bass, and A. D. Pitt, Phys. Rev. Lett. **58**, 2130 (1987).
[12]D. S. Chemla, I. Bar-Joseph, C. Klingshirn, D. A. B. Miller, J. M. Kuo, and T. Y. Chang, Appl. Phys. Lett. **50**, 585 (1987).
[13]H. Sakaki, H. Yoshimura, and T. Matsusue, Jpn. J. Appl. Phys. **26**, L1104 (1987).
[14]G. Trankle, H. Leier, A. Forchel, H. Haug, C. Ell, and G. Weimann, Phys. Rev. Lett. **58**, 419 (1987).
[15]P. T. Landsberg, Phys. Status Solidi **15**, 627 (1966).
[16]H. Yoshimura, T. Matsusue, and H. Sakaki, Extended Abstracts of the 19th Conference on Solid State Devices and Materials, Tokyo, 1987 (unpublished).
[17]A. Kastalsky, J. H. Abeles, and R. F. Reheny, Appl. Phys. Lett. **50**, 708 (1987).
[18]I. Bar-Joseph, J. M. Kuo, C. Klingshrin, G. Livesue, T. Y. Chang, D. A. B. Miler, and D. S. Chemla, Phys. Rev. Lett. **59**, 1357 (1987).
[19]C. Delalande, J. Orgonasi, J. A. Brum, G. Bastard, M. Voos, G. Weimann, and W. Schlapp, Appl. Phys. Lett. **51**, 1346 (1987).
[20]A. E. Ruckenstein and S. Schmitt-Rink, Phys. Rev. B **35**, 7551 (1987).
[21]G. E. W. Bauer and T. Ando, J. Phys. C **19**, 1553 (1986).

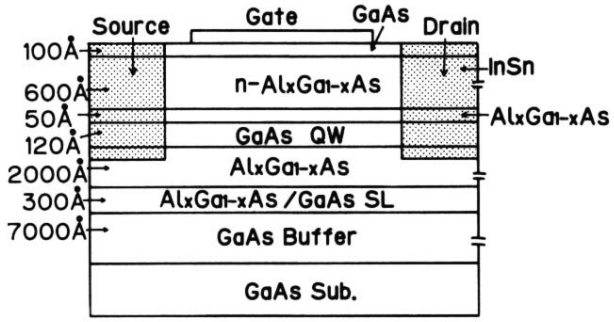

(a)

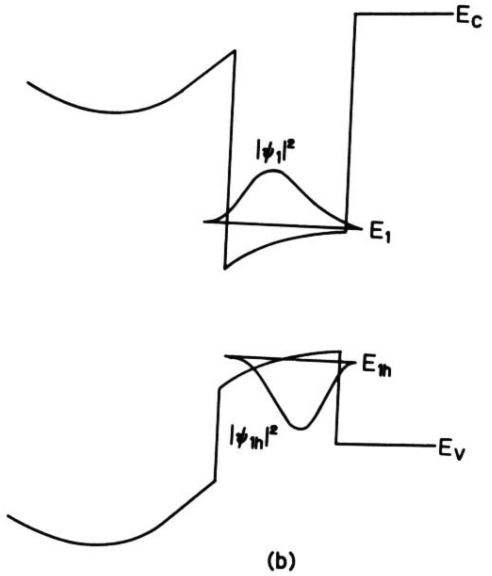

(b)

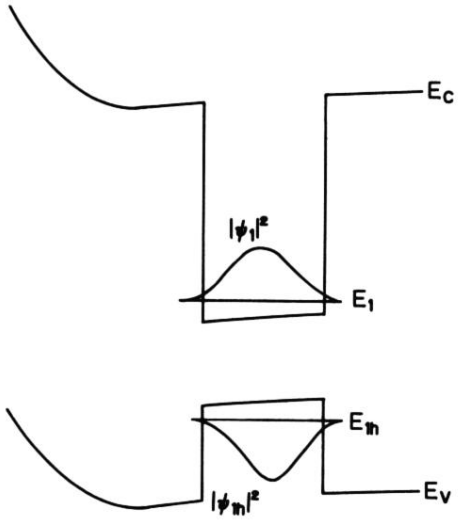

(c)

FIG. 1. The schematic structure of quantum-well FET (a) and the band bendings (b) and (c) at high and low electron concentrations.